

Electrochemical Reactivity of $\text{Li}_2\text{VOSiO}_4$ toward Li

A. S. Prakash,[†] P. Rozier,[‡] L. Dupont,[†] H. Vezin,[§] F. Sauvage,[†] and J.-M. Tarascon^{*,†}

*LRCs, Université de Picardie Jules Verne, UMR 6007 CNRS 33 rue Saint-Leu, 80039 Amiens, France,
CEMES/CNRS, Groupe Chimie des Matériaux Inorganiques, BP 4347, 31055 Toulouse Cedex 4, France,
and LCOM, CNRS UMR 8009 Bat C4, 59655 Villeneuve d'Ascq Cedex, France*

Received September 2, 2005. Revised Manuscript Received November 7, 2005

We report on the chemical/electrochemical reactivity of the insulating layered V-based silicate-phase $\text{Li}_2\text{VOSiO}_4$ toward Li. The silicate phase, made by a ceramic approach and consisting of 5–20 μm agglomerates, exhibits only a slight reactivity with Li in chemical or electrochemical reactions. By ball milling $\text{Li}_2\text{VOSiO}_4$ in the presence of carbon, we succeeded in preparing composites that reversibly react with 0.7 Li^+ per unit formula at an average voltage of 3.6 V vs Li^+/Li^0 . This electrochemical reactivity was chemically mimicked using NO_2BF_4 or Br_2 and LiI as oxidizing and reducing agents, respectively. Through a combination of X-rays and HRTEM measurements, we showed that the insertion–deinsertion mechanism is a two-phase process with poor kinetics. The delithiated phase crystallizes in space group $P4$ ($a = 6.206 \text{ \AA}$, $c = 4.5715 \text{ \AA}$), whereas the precursor lithiated phase crystallizes in $P4/nmm$ ($a = 6.366(9) \text{ \AA}$, $c = 4.456(6) \text{ \AA}$). Because silicates such as phosphates are cheap and can also be made redox-active by carbon coatings, they should not be overlooked as possible electrode candidates in future research.

Introduction

Because of the increasing demands for portable power sources to power electronics, the field of rechargeable batteries, and more specifically those batteries involving the Li ion, is enjoying great success. The search for better electrode materials has never been more intense. Historically, the number of candidate positive-electrode materials was relatively limited, because only materials with open-crystal structures together with good ionic and electronic conductivity were considered. More recently, the fascinating work on both carbon-coated LiFePO_4 ^{1,2} particles and nanoarchitected electrodes/current collectors³ showed that the scope of the search could be extended to materials without a particularly high electronic conductivity or high diffusion coefficient for lithium. Thus, a panel of previously disregarded materials belonging to the families of phosphates, sulfates, silicates, etc., are being revisited with some promising results, such as those obtained for LiMnPO_4 ⁴ or, just recently, on a not yet fully characterized $\text{Li}_2\text{FeSiO}_4$ phase.⁵ Besides the intensive work of Gaubicher et al.^{6,7} on VOXO_4 materials ($X =$

P, S), Patoux et al.⁸ investigated the $\text{Li}_x\text{TiOXO}_4$ family of compounds with $X = \text{Si}$ ($\text{Li}_x\text{TiSiO}_5$) and $X = \text{P}$ (Li_xTiPO_5), and found only electrochemical reactivity for Li for $X = \text{P}$ ($\Delta x = 0.6$ at 1.5 V vs Li^+/Li^0). As Ti is in its highest oxidation state (+IV) in these phases, Li could not be removed, which prevents the practical use of such materials in Li ion cells.

The present study falls within the context of such a general effort toward new potential-electrode materials, and focuses on the layered $\text{Li}_2\text{VOSiO}_4$ phase that, because of the presence of vanadium (+IV), should enable the removal of Li. Interestingly, this phase has been the subject of intense interest as a two-dimensional quantum Heisenberg anti-ferromagnetic prototype.^{9–11} The phase was first prepared in 1998 by Millet et al.¹² when the authors successfully substituted V for Ti in the lithium titanyl silicate-phase $\text{Li}_2\text{-TiOSiO}_4$. It crystallizes in the tetragonal system (space group $P4/nmm$). The structure can be viewed as being packed along the c -direction of $[\text{VOSiO}_4]_n$ sheets linked together by lithium ions located in distorted octahedral sites coordinated by oxygen (Figure 1a). Si is located in regular tetrahedral (Td) sites, whereas V^{4+} ions are located in square pyramidal (SP) sites, presenting four equivalent distances between V^{4+} and the oxygen of the basal plane, and a shorter distance between V^{4+} and the apical oxygen that corresponds to the typical

* To whom correspondence should be addressed. E-mail: jean-marie.tarascon@sc.u-picardie.fr.

[†] Université de Picardie Jules Verne.

[‡] CEMES/CNRS.

[§] LCOM.

- (1) Ravet, N.; Goodenough, J. B.; Besner, S.; Simoneau, M.; Hovington, P.; Armand, M. 196th Electrochemical Society Meeting, Hawaii, October 1999.
- (2) Huang, H.; Yin, S. C.; Nazar, L. F. *Electrochem. Solid-State Lett.* **2001**, *4* (10), A170.
- (3) Arico, A. S.; Bruce, P.; Scrosati, B.; Tarascon, J. M.; Schalkwijk, W. V. *Nat. Mater.* **2005**, *4*, 366.
- (4) Delacourt, C.; Poizot, P.; Morcrette, M.; Tarascon, J. M.; Masquelier, C. *Chem. Mater.* **2004**, *16*, 93–99.
- (5) Nytén, A.; Abouimrane, A.; Armand, M.; Gustafsson, T.; Thomas, J. O. *Electrochem. Commun.* **2005**, *7* (2), 156.
- (6) Gaubicher, J. Ph.D. Thesis, Université Pierre et Marie Curie, Paris, 1998.

- (7) Gaubicher, J.; Chabre, Y.; Angenault, J.; Lautie, A.; Quarton, M. *J. Alloys Compd.* **1997**, *262*, 34–38.
- (8) Patoux, S.; Masquelier, C. *Chem. Mater.* **2002**, *14* (12), 5057.
- (9) Melzi, R.; Carretta, P.; Lascialfari, A.; Mambrini, M.; Troyer, M.; Millet, P.; Mila, F. *Phys. Rev. Lett.* **2000**, *85* (6), 1318.
- (10) Kaul, E. E.; Rosner, H.; Shannon, N.; Shpanchenko, R.; Geibel, C. *J. Magn. Mater.* **2004**, *272–276* (Part 2 Special Issue), 922.
- (11) Rosner, H.; Singh, R. R. P.; Zheng, W. H.; Oitmaa, J.; Drechsler, S. L.; Pickett, W. E. C. A. K.-C.; Belle, C. *Phys. Rev. Lett.* **2002**, *88* (18), NIL_154–NIL_157.
- (12) Millet, P.; Satto, C. *Mater. Res. Bull.* **1998**, *33* (9), 1339.

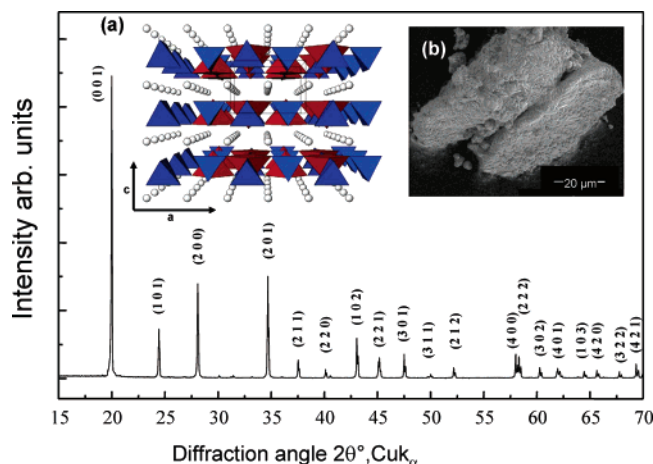


Figure 1. X-ray diffraction pattern of $\text{Li}_2\text{VOSiO}_4$ that crystallizes in a tetragonal structure (space group $P4/nmm$). The inset (left) shows a view of the $\text{Li}_2\text{VOSiO}_4$ down the b -direction. The layers of VO_5 square pyramids (dark/red polyhedra) shared corners with SiO_4 tetrahedra (shade/blue), and the Li ions between the layers are marked in circles. Inset (right) shows the scanning electron microscopy (SEM) image for prepared samples.

vanadyl bond. SiO_4 Td and VO_5 SP share corners, forming infinite chains along the $[100]$ direction. Adjacent chains that present VO_5 SP with the shortest vanadyl distance connect to each other in an alternating up and down manner along the $[010]$ direction by corner-sharing between SiO_4 and VO_5 SP, leading to the $[\text{VO}(\text{SiO}_4)]_n$ layers.

On the basis of recent advances toward designing conducting composites through the use of carbon-coating techniques, by either physical (ball milling) or chemical (polymer pyrolysis) means, we decided to investigate the electrochemical/chemical reactivity of the insulating $\text{Li}_2\text{VOSiO}_4$ phase toward Li. Using a ball milling approach, we succeeded in electrochemically deinserting/inserting Li from the layered insulating $\text{Li}_2\text{VOSiO}_4$ phase in a reversible way at a potential of 3.6 V vs Li, with a sustained capacity of 100 mAh g^{-1} .

Experimental Section

Characterization. The X-ray powder diffraction patterns were recorded on either a Scintag diffractometer ($\text{Cu K}\alpha$ radiation, $\lambda = 1.5418 \text{ \AA}$) or an Inel diffractometer ($\text{Cr K}\alpha$ radiation, $\lambda = 2.2897 \text{ \AA}$). The lattice parameters of the different phases encountered during this study were refined using the FullProf program.¹³ The morphology of the samples was studied by scanning electron microscopy (Philips SEM, FEG XL30). The high-resolution transmission electron microscopy images were taken with a Tecnai instrument. Compositions of the phases were determined using complementary techniques. Li and V were determined by atomic absorption spectroscopy (AAS, Perkin-Elmer Analyst 100), and Si:V ratios were obtained from the EDS on various spots using HRTEM. Finally, electron spin resonance (ESR) spectra were recorded at room temperature with an ELEXYS E580E X band spectrometer with an amplitude modulation of 5 G and a microwave power of 1 mW.

Positive electrodes were prepared by mixing 85 wt % active material and 15 wt % SP carbon as the electronic conductor. Swagelok type cells were assembled in an argon-filled glovebox with about 10 mg of the carbon–material mix, separated from the

negative electrode (lithium foil) by 2 sheets of fiber glass disks, and the entire setup was soaked with a LiPF_6 (1 M) solution in an ethylene carbonate (EC)/dimethyl carbonate (DMC) mixture (1:1, v/v). An aluminum current collector was used as the positive side to avoid electrolyte decomposition at high potential. Galvanostatic tests were conducted with a Mac Pile controller at a constant temperature of 25 $^\circ\text{C}$ unless otherwise specified.

For AC electrical conductivity measurements, we first pressed $\text{Li}_2\text{VOSiO}_4$ powders into pellets by means of uniaxial pressure (500 kg cm^{-2}). The resulting pellets were sintered under N_2 at 900 $^\circ\text{C}$ for 24 h, resulting in $\sim 76\%$ dense pellets. Careful control and polishing of the pellet surfaces was ensured before platinum deposition (sputtering) on opposite faces of the pellets. AC impedance measurements were done in air over the 130–300 $^\circ\text{C}$ temperature range using an Autolab PGSTAT20 impedance analyzer by applying a 350 mV amplitude in a frequency range of 1 MHz to 1 Hz.

Chemical analyses of lithium and vanadium were obtained by atomic absorption spectroscopy using acetylene–air and acetylene– NO_2 flames, respectively. In a typical experiment, about 35 mg of sample (LiVOSiO_4 or $\text{Li}_2\text{VOSiO}_4$) was dissolved in 3 mL of concentrated HCl. The solution was transferred to a volumetric flask, and was diluted to 500 mL. The instrument was precalibrated with four sets of standards of known concentration before the analysis.

$\text{Li}_2\text{VOSiO}_4$ Synthesis. The starting $\text{Li}_2\text{VOSiO}_4$ compound was prepared by a ceramic route. Stoichiometric amounts of Li_2SiO_3 (Aldrich) and VO_2 (Fluka) were placed in a stainless steel milling container, and were ball milled for 30 min under an Ar atmosphere using a SPEX 8000 shock-miller. The resulting powder was pressed into $12 \times 4 \text{ mm}^2$ pellets wrapped within platinum foil (to avoid direct contact of the reaction mixture with the silica tube); the pellets were placed in a fused silica tube that was then evacuated and sealed. The tube was heated at a rate of 4 $^\circ\text{C}/\text{min}$ to 925 $^\circ\text{C}$ for 24 h, and we then cooled it to room temperature by turning the furnace off. The resulting light brownish pellets were powdered prior to characterizing the structural and textural aspects. The powders were single-phased, as deduced from their X-ray diffraction pattern (Figure 1). Cell parameters, refined to $a = 6.366(9) \text{ \AA}$ and $c = 4.456(6) \text{ \AA}$, are in agreement with the reported literature values.^{12,14} The composition of the powder samples is deduced from complementary chemical titration and micro analysis (EDS) to be $\text{Li}_{1.95 \pm 0.1}\text{VOSiO}_4$. TGA measurements confirm that this phase is stable in air at ambient temperature, and does not pick up oxygen ($\text{V}^{4+} \rightarrow \text{V}^{5+}$) below 550 $^\circ\text{C}$. The powders consist of 1–4 μm agglomerates, as observed by scanning electron microscopy (Figure 1b). Such large agglomerates were thought to be responsible for the very low electrochemical activity (0.1 Li near 3.5 V at a $C/100$ rate) of the $\text{Li}_2\text{VOSiO}_4$ powders, even after the addition of a large percentage of carbon-conductive additives (about 15 wt %). The hint of electrochemical activity spotted near 3.6 V in the $E = f(x)$ curve was indicative of an active $\text{V}^{5+}/\text{V}^{4+}$ redox couple within the silicate, hence our desire to perform redox chemistry using classical oxidative and reductive agents such as NO_2BF_4 or Br_2 and LiI in acetonitrile, respectively.

Chemical Delithiation of $\text{Li}_2\text{VOSiO}_4$. Attempts to remove Li from $\text{Li}_2\text{VOSiO}_4$ were carried out by oxidative delithiation using NO_2BF_4 as an oxidizing agent. Typically, 0.5 g of $\text{Li}_2\text{VOSiO}_4$ powder was dispersed into a solution of 0.754 g of NO_2BF_4 in 50 mL of acetonitrile (Across, 99.5%). The reaction mixture was refluxed at 80 $^\circ\text{C}$ with continuous stirring inside an argon-filled glovebox, and the degree of completion was followed by withdraw-

(13) Rodriguez-Carvajal, J. *Physica B* **1993**, 192, 55.

(14) Ranagn, K. K.; Piffard, Y.; Joubert, O.; Tournoux, M. *Acta Crystallogr., Sect. C* **1998**, 54, 176.

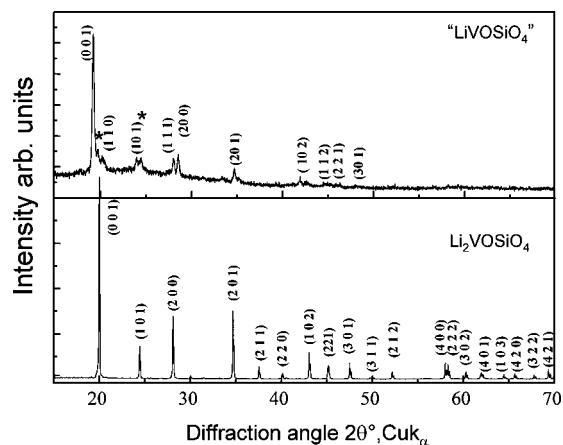


Figure 2. X-ray diffraction pattern of the chemically delithiated LiVOSiO_4 sample together with the hkl as deduced from microscopy. Asterisks (*) refer to some remaining peaks of the precursor phase indicative of a not fully completed reaction.

ing aliquots for testing. The aliquots were centrifuged; the resulting powders were then washed several times with acetonitrile, and were dried under vacuum prior to characterization by XRD. The supernatants were analyzed by AAS for Li and V. For the collected XRD patterns as a function of time, we limited the reaction time to 40 h, as beyond that time there was no change. Under such conditions, the recovered samples were yellowish with V:Si and Li:V ratios of 1 and 1.25, respectively, as deduced by EDS and AAS analysis. Longer reaction times were found to lead to decomposition reactions as evidenced by (i) color changes in both the solid and supernatant (e.g., powders gradually went from

yellowish to brownish, and the supernatant from orange to greenish, with increasing time), (ii) V:Si ratios less than 1, and (iii) the formation of reaction products with poorly defined XRD patterns.

As it is less oxidizing than NO_2BF_4 , Br_2 was used as a milder delithiation agent in order to better control the degree of delithiation. In a typical reaction, 0.5 g of a $\text{Li}_2\text{VOSiO}_4$ sample was refluxed with 50 mL of 1 vol % (0.4 mol/L) Br_2 solution in dry acetonitrile (Across, 99.5%) at 85 °C in air. From the evolution of the XRD, we deduced that the delithiation process of $\text{Li}_2\text{VOSiO}_4$ with Br_2 was reaching completion after 3 days. Its XRD pattern was better defined than those for samples obtained using NO_2BF_4 as an oxidizing agent, revealing drastic changes in the positions and relative intensities of the Bragg peaks compared to those of the precursor phase (Figure 2). Therefore, because of the weak intensity of the peaks except for the low-angle one ($2\theta = 29^\circ$), we could not satisfactorily determine the unit cell. TEM was used as a complementary technique to assign the set of Bragg reflections previously recorded by XRD. The effects of the chemical leaching are observed in the bright field image presented in Figure 3a with the creation of cracks within the initially massive particles. These cracks could be considered as being the trace of the departure of lithium from the pristine material. Although the observation of the particles at high magnification is quite difficult because of amorphization under the beam, several electron diffraction patterns were recorded. One of them (Figure 3b), showing a square symmetry, is assumed to be a characteristic plane for the $\text{Li}_x\text{VOSiO}_4$ cell, namely the c^* zone axis of a tetragonal cell having an a_{tetra} cell parameter roughly equal to 6.2 Å with no condition for the $(hk0)$ reflections. Another one (Figure 3c) shows a rectangular symmetry attributed to the b^* zone axis with a c_{tetra} cell parameter around 4.5 Å with no conditions for the $(h0l)$ reflections.

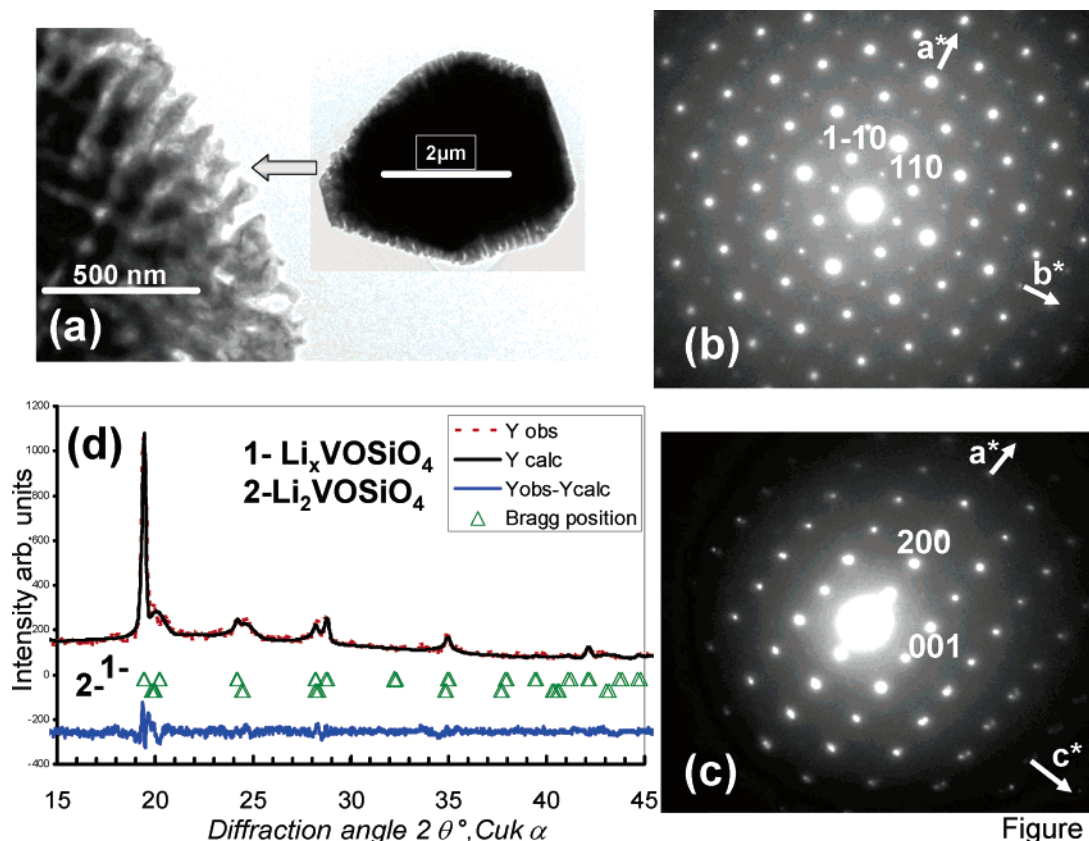


Figure 3

Figure 3. Transmission electron microscopy study of a chemically oxidized sample. showing (a) The bright field image, which shows that the initial massive particles crumble, inducing cracks due to lithium departure. (b, c) Two of the collected SAED patterns (along the c^* and b^* zone axis, respectively), which allow for determination of the cell parameters and space group of $\text{Li}_x\text{VOSiO}_4$. (d) The parameters were refined by pattern matching realized on the fully oxidized XRD diagram, leading to the following values: $a = 6.2063(8)$ Å, $c = 4.5714(9)$ Å, space group $P4$.

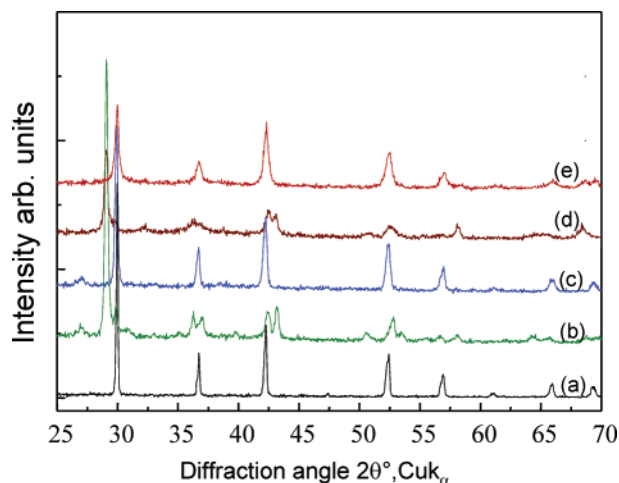


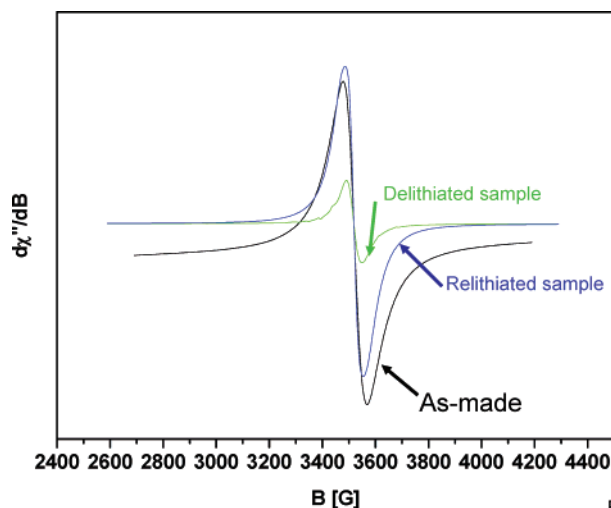
Figure 4. X-ray diffraction pattern showing (a) $\text{Li}_2\text{VOSiO}_4$ as prepared from the solid-state reaction; (b) chemical delithiation with Br_2 to give LiVOSiO_4 ; (c) chemical lithiation of LiVOSiO_4 with LiI to give $\text{Li}_2\text{VOSiO}_4$; (d) electrochemically delithiated LiVOSiO_4 ; (e) electrochemically lithiated $\text{Li}_2\text{VOSiO}_4$.

To test the validity of the cell parameters determined by electron diffraction ($a = b = 6.2 \text{ \AA}$, $c = 4.5 \text{ \AA}$, space group $P4$), we successfully realized a pattern matching (Figure 3d), on the basis of the XRD pattern recorded at the end of the chemical reaction. The matching was achieved when considering the sample to be a mixture of the starting $\text{Li}_2\text{VOSiO}_4$ compound and the $\text{Li}_x\text{VOSiO}_4$ delithiated compound. The refinement of the latter phase cell parameters leads to $a = 6.2063(8) \text{ \AA}$, $c = 4.5714(9) \text{ \AA}$, space group $P4$.

The decrease in the a -axis is consistent with the oxidation of V^{4+} into a smaller V^{5+} cation and, consequently, with a shrinkage within the $[\text{VOSiO}_4]_n$ layers. In contrast, the slight increase in the c -axis is less straightforward to explain, but could result from the competing effects of (i) a decrease in Li^+ screening between the $[\text{VOSiO}_4]_n$ layers, which would lead to an increase in the c -axis, and (ii) a decrease in the negative charge on the $[\text{VOSiO}_4]_n$ layers, which would lead to less repulsion between layers. The compositional analysis of the $\text{Li}_x\text{VOSiO}_4$ phase revealed its composition to be $\text{Li}_{1.18 \pm 0.1}\text{VOSiO}_4$. The delithiated samples were found to be air stable at least for a few days, but long-term stability and the effect of moisture were not explored.

To check whether the delithiated phase could re-intercalate Li, we simply used LiI as a reducing agent, because of the 3.6 V redox potential of the $\text{V}^{5+}/\text{V}^{4+}$ couple. $\text{Li}_{1.18}\text{VOSiO}_4$ (0.100 g) was added to a 100 cm^3 acetonitrile solution containing 0.1612 g of LiI (e.g., $2 \times$ stoichiometric). The reaction was conducted under reflux and with constant stirring. After a few minutes, the solution turns a reddish color, indicative of I_2 formation and Li insertion; after 15 h of reaction, we obtained a powder with an XRD pattern similar to that of the starting $\text{Li}_2\text{VOSiO}_4$ phase (Figure 4) with the composition $\text{Li}_{1.91 \pm 0.1}\text{VOSiO}_4$, suggesting that the delithiated phase has fully converted back. Because of the feasibility of this chemically driven insertion–deinsertion reaction, we further studied the electrochemical reactivity of $\text{Li}_2\text{VOSiO}_4$ toward Li.

In addition to chemical analysis, ESR measurements provide a nice way to monitor changes in the $\text{V}^{4+}:\text{V}^{5+}$ ratio within a compound because V^{5+} ($3d^0$) is not ESR active compared to V^{4+} ($3d^1$). The ESR spectra recorded at room temperature for the prepared $\text{Li}_2\text{V}^{4+}\text{OSiO}_4$ and for the chemically delithiated (Br_2) and relithiated (LiI) materials are shown in Figure 5. All the spectra show an isotropic signal with nonresolved hyperfine splitting of ^{51}V ($I = 7/2$) nuclear spin, indicative of the presence of V^{4+} . Therefore, the signal amplitude for the delithiated sample is



Fig

Figure 5. Experimental ESR spectra recorded at room temperature for the prepared $\text{Li}_2\text{VOSiO}_4$ sample and the chemically delithiated and relithiated samples.

considerably smaller than that of the prepared sample, suggesting a smaller amount of V^{4+} in this sample, and hence confirming the efficiency of the delithiation process. In contrast, the ESR signals practically superimpose for the prepared and relithiated samples. A rough estimate of the V^{4+} content in the delithiated sample was made as follows. For all of the collected ESR spectra, the V^{4+} surface-area peak was integrated and normalized to correspond to 1 V^{4+} atom of the prepared sample. Thus, by simple comparison, we could assign the number of V^{4+} ions in each spectrum. Values of 0.18 and 0.97 V^{4+} atom per unit formula were found for the delithiated and relithiated samples, respectively. Such values are in good agreement with those deduced from chemical analysis, further confirming the reversibility of the chemical deinsertion–reinsertion process. Two-dimensional pulse experiments using HYSORE (hyperfine sublevel correlation spectroscopy) were further performed on these samples in order to determine local structural changes in the V^{4+} , Li^+ , and Si^{4+} geometry upon Li deinsertion–reinsertion. By effectively measuring the hyperfine dipolar tensor \mathbf{T} of the ^{7}Li isotope, which has a $1/r^3$ dependency on the $\text{V}^{4+}\text{--Li}^+$ distance, we have shown that the \mathbf{T} value is decreased for the delithiated sample, suggesting an increase in the $\text{V}^{4+}\text{--Li}^+$ distance. This value was shown to convert back to its initial value for the relithiated sample, as expected. As we will describe elsewhere,¹⁵ we noted a difference regarding the Li–Si interaction that was not fully recovered for the relithiated sample.

Electrochemical Tests. To circumvent the poor electronic-conducting properties of the silicate phase, we pursued an approach similar to that recently applied with success to phosphates,^{16,17} consisting of either reducing the particle size or coating the particles with carbon. We did not succeed in preparing small particles of $\text{Li}_2\text{VOSiO}_4$ by soft-chemical routes, and therefore, concentrated on results obtained by the ball milling process in the presence of carbon to break agglomerates and simultaneously coat the particles with carbon.

Typically, for such experiments, about 1 g of $\text{Li}_2\text{VOSiO}_4$ powder together with 15 wt % carbon is loaded with a 7 g steel ball into a hardened stainless steel milling container. The hermetically sealed

(15) Vezin, H.; Prakash, A. S.; Morcrette, M.; Tarascon, J. M., Jr. *Phys. Chem.* Submitted for publication.

(16) Morcrette, M.; Wurm, C.; Masquelier, C. *Solid State Sci.* **2002**, *4*, 239.

(17) Morcrette, M.; Gillot, F.; Monconduit, L.; Tarascon, J.-M. *Electrochem. Solid-State Lett.* **2003**, *6* (4), A59–A62.

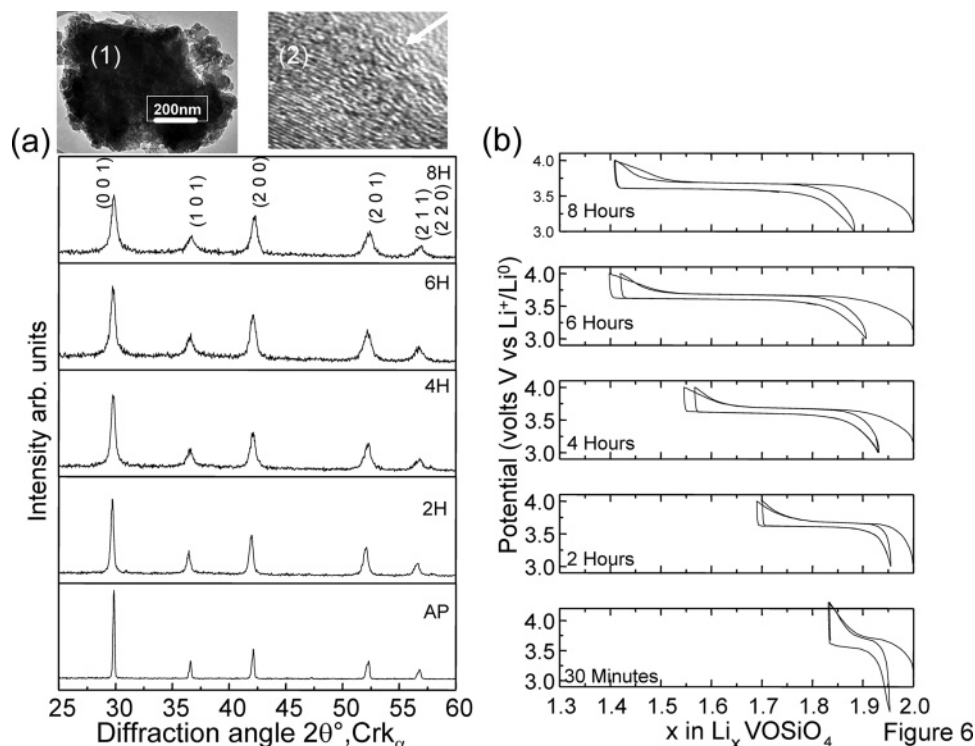


Figure 6. X-ray diffraction pattern of $\text{Li}_2\text{VOSiO}_4$ -C composites, ball milled in air for times ranging from 2 to 8 h (left) together with the corresponding voltage vs composition curves (right) collected at 25 °C at a rate of 1 Li in 25 h.

container is sequentially shaken for various lengths of time ranging from 1 to 6 h in a Spex 8000 miller with 15 min of interruption for every 30 min of milling to allow dissipation of heat developed during shock-induced milling. An immediate result of the ball-milling process (Figure 6a) with increasing milling time, as deduced from the XRD data and, more precisely, from the increase in the width of the Bragg peaks, is the breakdown of the agglomerates into particles as small as $0.5 \mu\text{m}$ after 6 h. The proof of an efficient carbon coating of the silicate particles resulting from the ball milling process was deduced from both bright field images that reveal a composite made of small crystallites and carbon balls (Figure 6, insets 1 and 2) and a high-resolution image (Figure 6a, inset 2) on the composite that nicely shows a well-crystallized particle embedded by carbon (white arrows). Milling times longer than 6 h did not lead to appreciable particle size reduction, but resulted in a considerable increase in Fe contamination ($2\theta = 68^\circ$) from the vial/ball abrasion.

The influence of ball milling on the electrochemical performance of $\text{Li}_2\text{VOSiO}_4$ -C composites is shown in Figure 6b. Overall, the longer the material is ball milled with carbon, the greater the capacity is. After ~ 300 min, additional ball milling becomes detrimental to capacity. Samples ball milled for 3 h showed a reversible capacity of 0.5–0.6 Li per formula unit.

Finally, through a survey of various electrode formulation parameters, namely in terms of the ratio of active material to conductive carbon and binder, the maximum Li that we succeeded in reversibly inserting–extracting in this compound at room temperature never exceeded 0.7 Li^+ per formula unit (Figure 7), even at a low rate ($C/50$). Therefore, sustained reversible capacities over at least 25 cycles (Figure 7, inset) were achieved. Alternatively, we attempted to enhance the Li uptake–removal amount by charging–discharging the cell at higher temperatures. At 75 °C (Figure 8), 0.85 Li^+ per unit formula can be removed at a rate of $C/25$, and 0.75 can be inserted back over the following discharge, leading to a reversible capacity of about 110 mA h g^{-1} , which

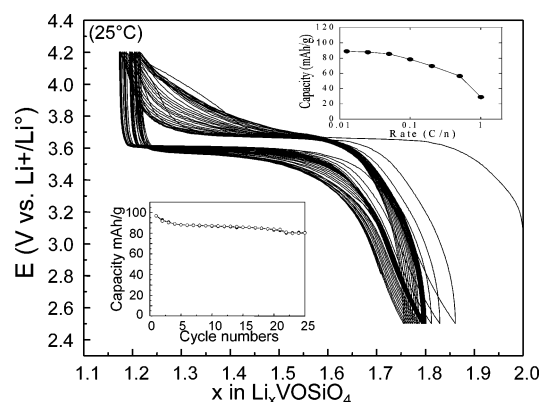


Figure 7. Potential vs composition curves. Insets: (i) the capacity vs cycle numbers and (ii) the power rate capability for $\text{Li}_2\text{VOSiO}_4/\text{Li}$ cells using $\text{Li}_2\text{VOSiO}_4$ -C composites that were ball milled for 6 h and cycled at room temperature at $C/50$. The capability data were taken by discharging the cell at various C/n rates down to 2.5 V after the cell had been charged to 4 V at a rate of $C/50$. Note that the regime C/n corresponds to the total amount of the capacity discharged in n hours.

decays (Figure 8, inset) faster upon cycling than at room temperature.

X-ray investigation found that the electrodes recovered from fully charged (up to 3.9 V; Figure 4d) and fully discharged (down to 3 V; Figure 4e) cells were found to nicely superimpose with those of the chemically delithiated samples in Figure 4b and the lithiated samples in Figure 4c, indicative that both the chemical and electrochemical approaches nicely mimic each other. A delithiation value greater than 1 could be attained at 75 °C with lower rates ($C/50$ or $C/100$), but on subsequent reduction, Li uptake was limited to about 0.65–0.75 Li per unit formula. This difference is an indication that there is a competing decomposition of the electrode material concomitant with Li removal, in agreement with the chemical delithiation experiment that also showed some degradation for long reaction times.

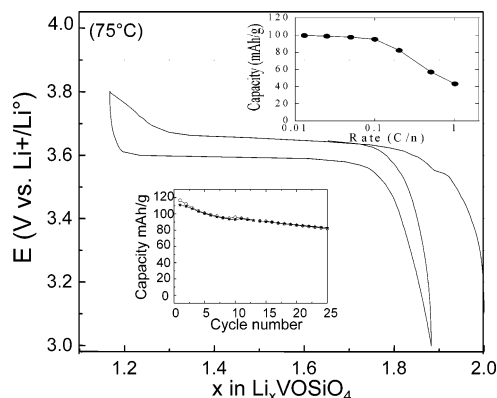


Figure 8. Potential vs composition curves. Insets: (i) the capacity vs cycle numbers and (ii) the power rate capability for $\text{Li}_2\text{VOSiO}_4/\text{Li}$ cells using $\text{Li}_2\text{VOSiO}_4\text{--C}$ composites that were ball milled for 6 h and cycled at 75 °C at $C/25$. The rate data were taken by discharging the cell at various C/n rates down to 2.5 V after the cell had been charged to 4 V at a rate of $C/25$.

Although the ball milling process does enhance the electrochemical capacity of $\text{Li}_2\text{VOSiO}_4$, our composite electrode still suffers from a lack of conductivity at high current density, as conveyed by the evolution of the discharge capacity vs the scan rate, from $C/1$ to $C/10$, reported in the insets of Figures 7 and 8. An increase in the discharge rate leads to a large decrease in capacity, showing that $\text{Li}_{2-x}\text{VOSiO}_4$ is strongly affected by kinetics; more than 60% of the initial capacity cannot be recovered at the C rate at 25 °C. Increasing the operating temperature to 75 °C slightly improves the rate capability, but it remains mediocre overall.

Because of the poor kinetics of the system, we have attempted to get a better insight into the $\text{Li}_2\text{VOSiO}_4$ transport properties. We carried out impedance spectroscopy measurements on a $\text{Li}_2\text{VOSiO}_4$ dense pellet (processed as described in the Experimental Section). The Nyquist spectra displayed a single semicircle with a pseudo-capacitance Y on the order of 10^{-11} F, corresponding to bulk conduction. Because the pellet had high impedance, we were able to evaluate its conductivity only for temperatures greater than 130 °C. Plots of $\log(\sigma T)$ vs $1000/T$ (Figure 9) gave a linear dependence that allowed us to calculate the activation energy for conduction according to the Arrhenius relation $\log(\sigma T) = \log(\sigma_0) - \Delta E/k_B T$. An activation energy (ΔE) of 0.96 eV was obtained. The extrapolated value of the RT conductivity was found to be very low, at around 8×10^{-15} S/cm (assuming that no break in the dependence occurs at lower temperature). Such large room-temperature resistance together with the large activation energy is consistent with the poor electrochemical performance of this electrode material in terms of rate capabilities, as previously described. To bypass such kinetic limitations, attempts at reducing particle size together with designing better electronic coatings for the particles are underway. Such approaches hold promise, as they were shown to be successful in improving the electrochemical performance of the olivine LiMnPO_4 phase¹⁸ that shows a $\Delta E \approx 1.1$ eV and a $\sigma_{25} \approx 9 \times 10^{-16}$ S/cm, similar to that measured for $\text{Li}_2\text{VOSiO}_4$.

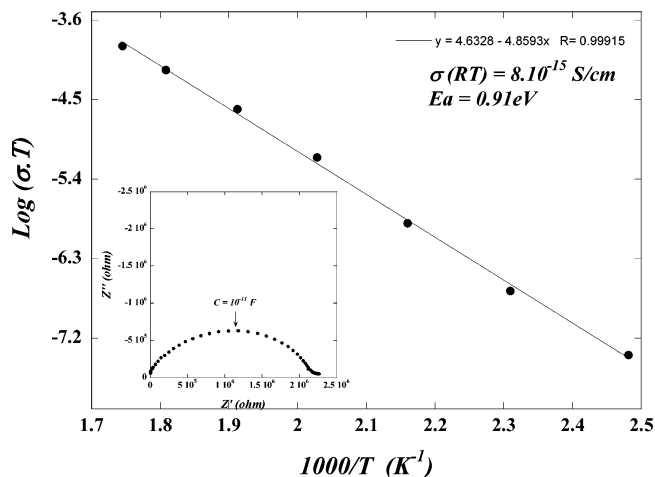


Figure 9. Temperature-dependent conductivity plots for $\text{Li}_2\text{VOSiO}_4$ pellets. The open symbols are experimental data, and solid lines through the open symbols are fit to the Arrhenius equation.

Conclusions

We have reported the electrochemical activity of the insulating layered $\text{Li}_2\text{VOSiO}_4$ phase toward Li as well as its aptitude for a reversible capacity of 0.6 Li per unit formula at an average voltage of 3.6 V when ball milled with carbon. Because of its weak capacity and limited kinetics, this material is not suitable for practical applications, but it does have pedagogical value. It reinforces the notion that materials active toward Li require neither a particularly high electronic conductivity nor a high diffusion coefficient for lithium when ball milled in the presence of carbons. The benefit of such a process is believed to be nested, as deduced by TEM observations, in the cumulative effects of particle size reduction together with the formation of new interfaces that favor efficient carbon coatings. This work, in conjunction with the previous study by Nytén et al.⁵ on the electrochemical reactivity of $\text{Li}_2\text{FeSiO}_4$ toward Li, clearly indicates that silicates, although insulating, should not be banished from the list of potentially attractive electrode materials. Furthermore, in light of such findings, other insulating materials with a type of structure similar to that of the layered silicate, such as, for instance, $\text{K}_2\text{V}_3\text{O}_8$, are worth reinvestigating, as is presently being done. Finally, although it is beyond the scope of this paper, this work opens up an interesting set of materials for the field of frustrated magnetic systems, and more specifically on the influence of injecting a diamagnetic V^{5+} ion (e.g., diluting the spins) in a quantum Heisenberg antiferromagnetic prototype, which is being experimentally explored.

Acknowledgment. The authors thank D. W. Murphy, C. Masquelier, M. Morcrette, D. Larcher, C. Delacourt, and C. Surcin for helpful discussions.

CM051986K

(18) Delacourt, C.; Laffont, L.; Bouchet, R.; Wurm, C.; Leriche, J.-B.; Morcrette, M.; Tarascon, J.-M.; Masquelier, C. *J. Electrochem. Soc.* **2005**, *152* (5), A913–A921.